Wave trapping and E x B staircases

Xavier Garbet, O Panico, R Varennes, C Gillot, Guilhem Dif-Pradalier, Y Sarazin, V Grandgirard, P Ghendrih, L Vermare

Wave trapping and $E \times B$ staircases

X. Garbet[1], O. Panico[1,2], R. Varennes[1],
C. Gillot[1], G. Dif-Pradalier[1], Y. Sarazin[1],
V. Grandgirard[1], P. Ghendrih[1], L. Vermare[3]

[1]CEA, IRFM, Saint-Paul-lez-Durance, F-13108, France.

[2] Département de Physique, ENS de Lyon / Université Lyon 1, 46 Allée d'Italie, F-69364 Lyon Cedex 07, France.

[3]LPP, CNRS, Ecole polytechnique, UPMC Univ Paris 06, Univ. Paris-Sud, Université Paris-Saclay, Sorbonne Universités, 91128 Palaiseau, France.

January 5, 2021

Abstract

A model of $E \times B$ staircases is proposed, based on a wave kinetic equation coupled to a poloidal momentum equation. A staircase pattern is idealised as a periodic radial structure of zonal shear layers that bound regions of propagating wave packets, viewed as avalanches. Wave packets are trapped in shear flow layers due to refraction. In this model an $E \times B$ staircase motif emerges due to the interaction between propagating wave packets (avalanches) and trapped waves in presence of an instability drive. Amplitude, shape, and spatial period of the staircase $E \times B$ flow are predicted as functions of the background fluctuation spectrum and the growth rate of drift waves. The zonal flow velocity radial profile is found to peak near its maxima and to flatten near its minima. The optimum configuration for staircase formation is a growth rate that is maximum at zero radial wave number. A mean shear flow is responsible for a preferential propagation speed of avalanches. It is not a mandatory condition for the existence of staircase solutions, but has an impact on their spatial period.

1 Introduction

Zonal flows play an important role in turbulence self-regulation and thereby on turbulent transport in magnetised plasmas [1, 2, 3] (see also [4] and references therein for an overview). The dynamics of zonal flows is often computed by solving a poloidal momentum equation coupled to a wave kinetic equation. In this description, zonal flows are driven by the divergence of the turbulent Reynolds stress, and damped by collisional friction or viscosity, or turbulent hyper-viscosity. The Reynolds stress is related to a moment of the wave action density, itself solution of a wave kinetic equation [5]. Hence the wave kinetic equation is a powerful tool to study the back-reaction of zonal flows on the turbulence background. Other routes are possible, like using a 4 wave model that couples drift waves to a zonal flow [6, 7], then extended to a 3 wave model for generation of Geodesic Acoustic Modes [8]. Several derivations of the wave kinetic equation exist [9, 10, 11], including recent extensions based on the Wigner-Moyal equation [12, 13, 14] or a variational approach [15]. In most cases, the regime of interest addresses a population of zonal flows with random phases that scatter drift waves, which in turn drive zonal flows via the Reynolds stress. A quasi-linear theory can then be used to solve the wave kinetic equation and predict the growth rate of zonal flows.

Zonal flows play a major role in the dynamics of "$E \times B$" staircases, which are self-organised turbulent states observed in a number of gyrokinetic simulations [16, 17, 18, 19, 20, 21]. Similar patterns were observed in simulations of a reduced 2D model of interchange turbulence [22] and also 2D ion temperature gradient (ITG) turbulence [23]. Some experimental observations were found consistent with a staircase phenomenology [24, 25, 26]. An "$E \times B$" staircase can be described schematically as an array of shear flow layers that bound regions of propagating avalanches. Avalanches can be viewed as mesoscale transport events [27, 28, 29, 30, 31] (see also overviews [32, 33]). Hence a staircase pattern can be idealised as a quasi-static and quasi-periodic structure of zonal shear layers that surround avalanching areas. This is to be contrasted with the common picture of a bath of random time-dependent zonal flows in strong interaction with turbulent vortices. Of course both situations can coexist, i.e. random zonal flows tightly coupled to a turbulent bath, which live in between quasi-static shear layers. Quasi-periodic does not mean here sinusoidal. Indeed shear layers materialise as velocity bumps in a sketchy representation of a staircase pattern (see figure 1 in [18]). In practice, the shape of shear layers is quite irregular. Moreover zonal layers are often observed to drift slowly in the radial direction and may merge or diverge on long time scales compared with avalanche spreading times. This complex dynamics has been studied in detail in [34], and is not modelled in the present work, which is rather focused on the short time scales dynamics of staircases.

Several open issues subsist in the understanding of staircase pattern formation and sustainment, which were identified and summarised in [35]. One pending issue is the pattern selection processes that determine the intensity and width of the shear layers, and their spatial period. Also the dependence on the initial state on plasma parameters is not well understood. Another vivid question is whether avalanches participate in the staircase build-up, or whether their confinement is a mere consequence of zonal flow layering. Finally the mean flow is possibly a key player. Its interplay with staircase shear layers remains to be clarified. In fact the definition of a mean flow is somewhat debatable, especially in the limit of static shear layers where the difference between zonal and mean flows is tenuous. The simplest option in a tokamak is to define a "mean flow" as the one that would be obtained without turbulence, so essentially the one predicted by neoclassical theory combined with a force balance equation and a prescribed toroidal velocity. An alternative is to define the mean flow as the result of neoclassical viscous damping *and* turbulent drive, but without accounting for the corrugations associated with the staircase shear layers. This is equivalent to a radially coarse-grained velocity profile.

Since the existing models of zonal flow formation and avalanche generation did not seem to answer these interrogations, radically different approaches have been proposed and documented in the literature. One very first attempt was a reduced model for the mean temperature inspired from fluid-like models for jam formation in traffic flow [36, 37]. In this model, jams are temperature corrugations interspersed with regions where blobs and holes (avalanches) propagate. The formation of shear layer is merely a consequence of temperature corrugations. An alternative model has been proposed in [38, 39, 35]. In this line of research, a set of reduced 1D PDEs has been developed that describes the dynamics of drift waves coupled to zonal flows. The initial version of the model is based on the Hasegawa-Wakatani model [40] of drift waves, and involves 3 evolution equations for the density, vorticity and turbulence intensity. Bi-stability is introduced in the model via the non linear dependence of the mixing length on density and vorticity gradients, and turbulence intensity. The resulting dynamics present many features consistent with staircases as observed in gyrokinetic simulations. One striking result is the sensitivity of the staircase formation on the density gradient, and not that much on the zonal $E \times B$ flow shearing. Turbulence spreading (avalanches) play some role, but is not critical. The evolution of the staircase depends on both mean and zonal feedback on turbulence via shearing. Though promising, this class of models relies on a bistable character that remains to be demonstrated in 5D gyrokinetic simulations. Another approach was proposed in [20], where the staircase

builds up through a series of steps that can be summarised as follows. The initial growth of an ITG mode induces a temperature relaxation. A corrugated zonal flow appears due to momentum balance equation. This zonal flow is responsible for a split of the initial large scale ITG mode into smaller eddies. The eddies realign to produce another large scale structure, i.e. an avalanche, and the process is iterated again. The presence of a mean flow is essential to allow a preferential direction of avalanches via a realignment of turbulent eddies ("elevator" effect). The propagation speed is in fact related to the gradient of the mean flow. So in this process, both mean flow and avalanches are key ingredients in the staircase build-up. The reason why the process leads to a steady state, with a finite number of shear layers, remains to be clarified. Finally a recent work has proposed a model of staircases based on coupled non-linear oscillators governed by a generalized non linear Schroedinger equation with a sub-quadratic power non-linearity [41]. In essence it computes the event size distribution of avalanches in interaction with a static array of shear layers. The predicted distribution has been successfully compared with gyrokinetic simulations. No prediction though is provided for the number of shear layers in a staircase, and their dynamical evolution.

The present model remains within the traditional approach of a wave kinetic equation coupled to a zonal flow momentum equation. The rationale can be roughly described as follows. It is known that the wake kinetic equation coupled to a zonal momentum conservation equation admits a class of coherent solutions [42, 43]. Some of these solutions are static and radially periodic [43]. Also wave packets that propagate radially at their group velocity can be viewed as a proxy for avalanches (as suggested in [42]). A staircase pattern can then be viewed as a periodic and static radial array of zonal flows that coexist with moving wave packets. It is also known that a periodic array of zonal shear layers produces an island structure in the wave phase space (position, wave number). For drift waves, a zonal flow maximum is generically associated with the island O point, while a flow minimum is an X point [14]. An X point is topologically different from an O point, suggesting different behaviours. Hence it is expected that flow minima and maxima do not behave in the same way. In particular, wave packet trapping occurs near flow maxima, whereas passing wave packets (avalanches) are expected to "erode" the island X-point, i.e. flow minima. A staircase-like pattern can therefore be anticipated, where turbulent wave packets are trapped within zonal shear layers, while avalanches propagate in between. Traditional models based on random eddies do not address the physics of wave trapping. However adding wave trapping does not grant the existence of staircase solutions. Non linear solutions of the wave kinetic/momentum equations with wave trapping have been found in a seminal work by Kaw and co-workers [44]. Solutions were found where coherent zonal

flows propagates radially together with drift waves that are trapped in the zonal structure. The same methodology was used for Geodesic Acoustic Modes [45, 15]. It was shown that GAMs can be non-linearly destabilised by wave trapping. The present work rather aims at proving the existence of static zonal periodic solutions, which coexist with moving avalanches. In [44], the structure of the zonal potential that enters the wave kinetic equation was chosen on the basis of general considerations, thus leaving some freedom in the nature of the solutions, which appeared to be solitons, shocks or wave trains. In fact solutions are strongly constrained by non linear wave-wave interactions that appear through a Boltzmann-like differential operator in the wave kinetic equation. This important point is clarified in the present work. It appears that staircase solutions are possible only if a turbulence drive is accounted for in combination with wave trapping. Values of the staircase flow amplitude, shape, and spatial period can then be computed. One important outcome is the radial localisation of the zonal flow velocity near its radial maxima (O points). Finally a mean shear flow is needed to explain the preferential propagation speed of avalanches. It favours the onset of a staircase but is not a necessary condition for the existence of staircase solutions. It is stressed that the dynamics of shear layers is not addressed here, in particular the complex splitting/merging behaviour. The calculation is done here for conventional drift waves, an already challenging task. However it can be extended to ITG modes in tokamaks by using a formalism recently developed by Gillot and co-workers [15].

The remainder of the paper is organised as follows. The section 2 presents the basics of drift waves, and the model to be solved. Section 3 reminds the notion of wave trapping and some general solutions of the wave kinetic equation. General conditions for getting staircase-like solutions are detailed in section 4. The specific case of a wave-wave interaction operator that is diffusive, in presence of a turbulence drive, is addressed in section 5. A discussion follows in section 6, and conclusions are drawn in section 7.

2 Zonal flows coupled to drift waves

2.1 Brief reminder on drift waves and zonal flows

Drift waves are ubiquitous in magnetised plasmas. In the simplest model, a Cartesian set of coordinates (x, y, z) is used. The magnetic field $\mathbf{B}$ is uniform, directed along the z direction. The unperturbed density N_{eq} depends on x only, the electron temperature T_e is constant, and the ion temperature vanishes (see figure 1). All quantities are supposed to depend on (x, y) only , i.e. the model is 2-dimensional. A self-consistent model is built by coupling the ion continuity equation, a Boltz-

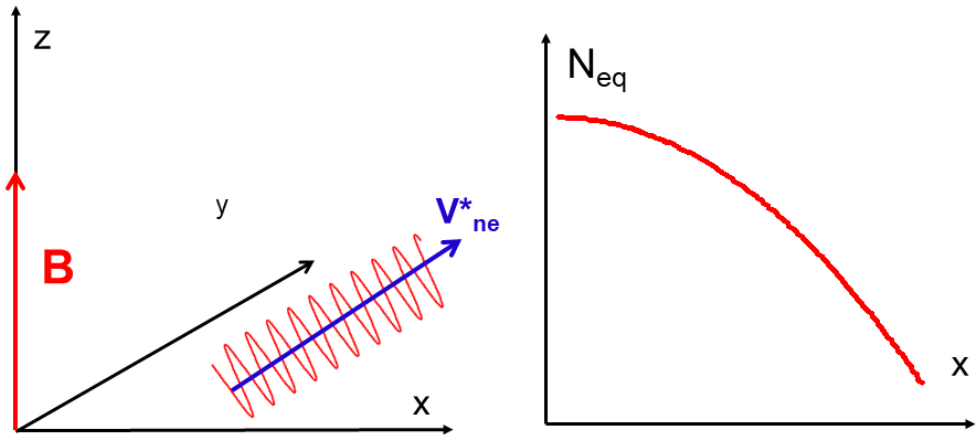

Figure 1: Geometry and schematics of a drift wave.

mann electron density response, and the charge quasi-neutrality constraint. This leads to the Hasegawa-Mima equation [46]. The "modified" Hasegawa-Mima equation accounts for the vanishing response of the perturbed electron density to zonal flows, and reads

$$\left(\frac{\partial}{\partial t} + \mathbf{V}_E \cdot \nabla\right) \Omega + \frac{\partial \phi}{\partial y} = 0 \tag{1}$$

where $\Omega = \phi - \bar{\phi} - \nabla_\perp^2 \phi$ is the potential vorticity. The same equation holds for Rossby waves in the stratified atmosphere of rotating planets, ϕ being the stream function of the incompressible fluid [47]. All lengths are normalised to the ion "sound" gyroradius $\rho_s = \frac{\sqrt{m_i T_e}}{eB}$. The field ϕ is the electric potential normalised to $\frac{T_e}{e}\frac{L_n}{\rho_s}$ (L_n is the density gradient length), $\bar{\phi}$ its average over the periodic direction y. Also $\mathbf{V}_E = \hat{\mathbf{e}}_z \times \nabla\phi$ denotes the $E \times B$ electric drift velocity, normalised to the electron diamagnetic velocity $V_* = \frac{T_e}{eBL_n}$. Hence the time unit is $\rho_s/V_* = L_n/c_s$. Drift waves are marginally stable in this model. Instabilities can be introduced by using the 2-field Hasegawa-Wakatani model [40]. It can also be made unstable in a simpler way by slightly modifying the Boltzmann electron response ("$i\delta$ model") ,

which leads to a modified potential vorticity $\Omega = \phi\,(1 - i\delta_e) - \bar{\phi} - \nabla_\perp^2 \phi$, where δ_e is suitably defined via its Fourier transform $\delta_{\mathbf{k}}$ [48, 49]. Instabilities grow whenever $k_y \delta_{\mathbf{k}} > 0$.

2.2 Wave kinetics and force balance equation

The Hasegawa-Mima equation, and its variants, is usually solved numerically. However the dynamics of drift waves in interaction with zonal flows can be described by a wave kinetic equation, exact for the part related to the interaction with zonal flows provided that the zonal flows wave numbers are much smaller than those of drift waves. It takes the form [11]

$$\frac{\partial N}{\partial t} - \{H, N\} = \mathcal{D}\,[N] \tag{2}$$

where $N(\mathbf{x}, \mathbf{k}, t)$ is a wave action density, a real-valued function defined for drift waves as

$$N(\mathbf{x}, \mathbf{k}, t) = \sum_{\mathbf{p}} \Omega\left(\mathbf{k} + \frac{\mathbf{p}}{2}, t\right) \Omega^*\left(\mathbf{k} - \frac{\mathbf{p}}{2}, t\right) e^{i\mathbf{p}\cdot\mathbf{x}}$$

Here $\Omega(\mathbf{k}, t) = (1 + k_\perp^2)\phi(\mathbf{k}, t)$ is the Fourier transform of the potential vorticity for $k_y \neq 0$ drift waves, $(\mathbf{x}, \mathbf{k})$ the position and wave number of wave packets. Assuming a statistical translational invariance of the background fluctuations, an alternative definition is obtained via the shifts $\mathbf{k} + \frac{\mathbf{p}}{2} \to \mathbf{k}$ and $\mathbf{k} - \frac{\mathbf{p}}{2} \to \mathbf{k} - \mathbf{p}$. This alternative version is more convenient to compute the Reynolds stress. The Poisson bracket reads

$$\{H, N\} = \frac{\partial H}{\partial \mathbf{x}} \cdot \frac{\partial N}{\partial \mathbf{k}} - \frac{\partial H}{\partial \mathbf{k}} \cdot \frac{\partial N}{\partial \mathbf{x}}$$

The wave "Hamiltonian" reads

$$H = \omega_{\mathbf{k}} + k_y V(x, t) \tag{3}$$

where $\omega_{\mathbf{k}}$ is the linear frequency of a drift wave, k_y its poloidal wave number. The zonal flow velocity $V(x, t)$, directed in the "poloidal" periodic direction y, depends exclusively on the "radial" coordinate x. The drift wave frequency $\omega_{\mathbf{k}}$ is

$$\omega_{\mathbf{k}} = \frac{k_y}{1 + k_x^2 + k_y^2}$$

It was stressed by Parker [50] and subsequent authors [13, 14] that a $\partial_{xx} V(x, t)$ term should be included in the expression of the angular frequency $\omega_{\mathbf{k}}$, and also an extra term in the r.h.s. of the wave kinetic equation. These terms matter for

high wave number zonal flows, since they avoid an "ultra-violet" catastrophe when computing their growth rate. In other words they provide damping at high wave numbers. The typical wave length of shear layers in a staircase is much larger than the scale of background eddies (from [18] the distance between shear layers, i.e. the staircase period, is around $40\rho_s$). Hence these terms are neglected in this model. Finally the differential operator $\mathcal{D}[N]$ that appears in the right hand side of Eq.(2) covers the non-linear physics of wave-wave coupling. It plays the same role as the collision operator in a conventional kinetic equation. The operator $\mathcal{D}[N]$ is in principle non linear in N. An explicit expression can be found by using a random phase approximation, but it remains quite intricate and difficult to handle [11]. We will resort to approximate forms in the following.

The time evolution of the poloidal velocity of zonal flows is given by a momentum equation

$$\frac{\partial V}{\partial t} = \mathcal{F} - \nu V + \mu \frac{d^2 V}{dx^2} \tag{4}$$

where $\mathcal{F}(x,t)$ is the force exerted by the drift wave turbulent background, i.e. minus the divergence of the Reynolds stress. The coefficients ν and μ correspond to damping terms, associated respectively with neoclassical friction forces and flow viscous damping [43]. The force $\mathcal{F}$ is related to the wave action density via the equation

$$\mathcal{F} = \int \frac{d^2\mathbf{k}}{4\pi^2} \frac{1}{\left(1 + k_x^2 + k_y^2\right)^2} k_x k_y \frac{\partial N}{\partial x} \tag{5}$$

The set of equations Eqs.(2,4,5) describes the dynamics of drift waves coupled to zonal flows.

3 BGK structure in the phase space

3.1 Normalised wave kinetic equation

We consider a background of drift wave packets, treated as quasi-particles in the wave kinetic approach. Wave packets propagate at group velocity v_g in the "radial" direction x. These wave packets are considered as proxies for avalanches. They interact with quasi-static zonal flows, whose poloidal velocity depends on x only. There is no dependence on the y coordinate, so that wave numbers k_y are invariants of motion. For a periodic zonal flow velocity $V(x)$, the contour lines of the Hamiltonian Eq.(3) exhibit a characteristic island (or "cat-eye") shape near the line $k_x = 0$ (see Fig.2). An island can be seen as special case of Bernstein-Greene-Kruskal (BGK) coherent structure [51]. Another virtual island appears at $k_x \to \infty$, but plays little role here. The analysis is therefore restricted to the

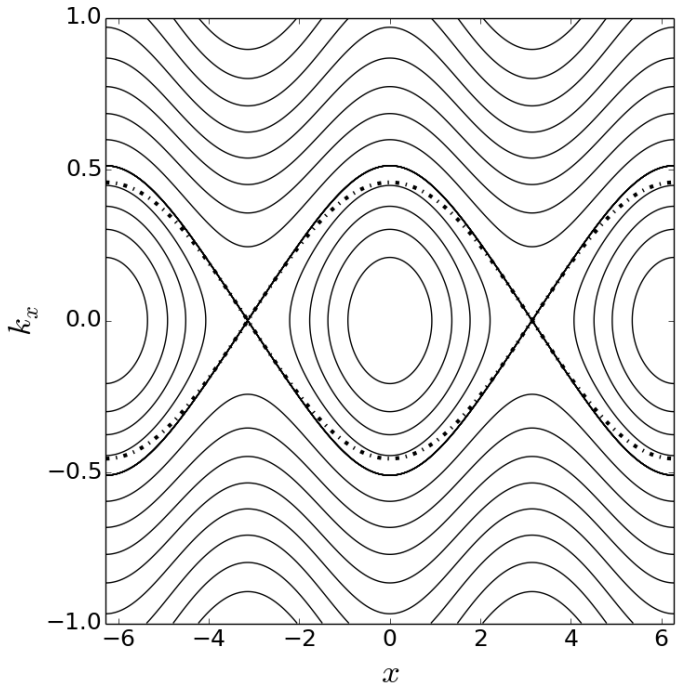

Figure 2: Contour lines of the Hamiltonian for a periodic zonal flow $V(x) = 0.1\cos(x)$ and a poloidal wave number $k_y = 0.1$. The dashed dotted line shows the separatrix when using a Taylor development of $\omega_{\mathbf{k}}$ near $k_x = 0$. The thick solid line is the exact separatrix.

vicinity of the wave number $\bar{\mathbf{k}} = (0, k_y)$, i.e. the domain where $k_x \ll k_y$. The Hamiltonian can be safely shifted by a frequency $\omega_{\bar{\mathbf{k}}} = k_y/(1 + k_y^2)$ since k_y is an invariant of motion. It is thus recast as

$$H = -k_y \left(\frac{1}{2} C_k k_x^2 - V(x) \right)$$

where the coefficient C_k depends on k_y only (quantities that depend on k_y only are labelled with a subscript 'k' throughout the paper), and

$$C_k = \frac{1}{(1 + k_y^2)^2}$$

The parabolic approximation near $k_x = 0$ provides a reasonable description of the island shape, as seen in Fig.2. Note that the condition $k_x \ll k_y$ does not necessarily contradicts the assumption of large scale zonal flow compared with the turbulent eddy size. The island width is $2\sqrt{(2V_+ - V_-)/C_k}$, where V_- and V_+

are the minima and maxima of the zonal flow velocity. Hence the condition of validity is a typical wave number of zonal flows smaller than $2\sqrt{(2(V_+ - V_-)/C_k}$, itself smaller than k_y. The wave kinetic equation Eq.(2) can be formulated in a convenient form

$$C_k k_y \{w, N\} = \mathcal{D}[N] \tag{6}$$

where $v = V/C_k$ is a normalised zonal flow velocity, and w a reduced Hamiltonian

$$w(x, k_x) = \frac{1}{2}k_x^2 - v(x) \tag{7}$$

3.2 Quasi-linear solution

It is interesting to connect the present approach with previous studies by considering velocity perturbations of the form

$$V(x) = V_q e^{iqx} + c.c.$$

A Krook dissipation operator is employed

$$\mathcal{D}[N] = -\eta_k (N - N_{eq}) \tag{8}$$

where

$$N_{eq}(\mathbf{k}) = N_{eq}\left(\bar{\mathbf{k}}\right) + \left.\frac{\partial N_{eq}}{\partial k_x}\right|_{\mathbf{k}=\bar{\mathbf{k}}} k_x \tag{9}$$

is an expansion of the unperturbed wave action density near $\bar{\mathbf{k}} = (0, k_y)$, and $\eta_k > 0$ is a dissipation rate. The wave action perturbation reads

$$N(x, \mathbf{k}) = N_{eq}(\mathbf{k}) + N_q(\mathbf{k}) e^{iqx} + c.c.$$

The linearised solution of the wave kinetic solution Eq.(6) reads

$$N_q = -\frac{k_y q V_q}{-q v_{g\mathbf{k}} + i\eta_k} \left.\frac{\partial N_{eq}}{\partial k_x}\right|_{\mathbf{k}=\bar{\mathbf{k}}} \tag{10}$$

where

$$v_{g\mathbf{k}} = k_y \left.\frac{\partial^2 \omega_{\mathbf{k}}}{\partial k_x^2}\right|_{\mathbf{k}=\bar{\mathbf{k}}} k_x$$

is the drift wave group velocity. Hence Eq.(10) agrees with the traditional linear solution of the wave kinetic equation [5] in the static limit. Let us consider a bath of drift waves with random phases, allowing the use of a quasi-linear theory, and restrict the analysis to the dissipative limit $|q v_g| \ll \eta_k$. Plugging the linear

solution for each q mode in the Reynolds stress yields a quasi-linear zonal force [5], reproduced here for self-containedness

$$\mathcal{F}_q = q^2 \int \frac{dk_y dk_x}{4\pi^2} \frac{k_y^2}{\left(1+k_x^2+k_y^2\right)^2} \left(-k_x \frac{\partial N_{eq}}{\partial k_x}\right) \frac{1}{\eta_k} V_q \tag{11}$$

According to the momentum equation Eq.(4), the force $\mathcal{F}_q$ provides the growth rate of the zonal flow in absence of friction and viscosity. A zonal instability appears whenever

$$-k_x \frac{\partial N_{eq}}{\partial k_x} > 0 \tag{12}$$

over a significant part of the spectrum. Also the force is anti-diffusive since $\mathcal{F}_q \sim +q^2 V_q$ [5].

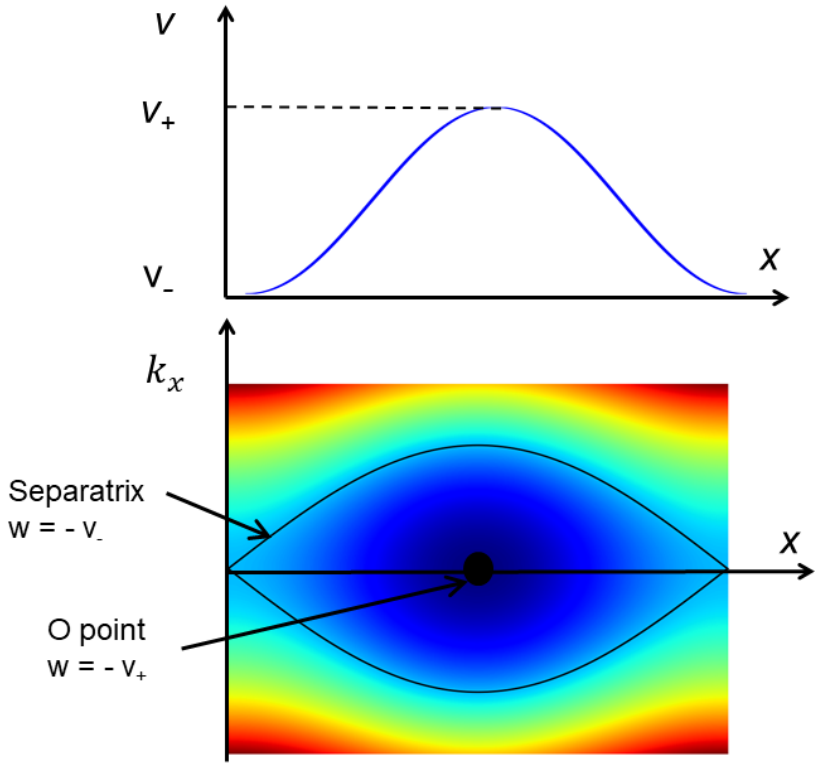

Figure 3: Island shape for a sinusoidal flow profile $v = cos(x)$. The black solid line is the island separatrix $w = -v_-$ and the black-faced circle is the O point $w = -v_+$.

3.3 Wave trapping

Another class of solutions is investigated, where drift waves radially bounce back and forth due to their refraction on the zonal flow velocity. This situation was studied by P.K. Kaw et al. [44]. The signature of wave trapping is a change of sign in time of the radial wave number k_x. The expression Eq.(7) of the Hamiltonian w reflects this physics. It is similar to the Hamiltonian associated with the motion of a particle with momentum k_x in a potential $-v(x)$. Bouncing occurs at position $x_0(w)$ such that $w = -v(x_0)$ admits a solution $x_0(w)$ (multiple solutions are possible). The w iso-lines $w(x, k_x) = cte$ draw a traditional island shape for functions v that exhibit a minimum v_- and a maximum v_+ (see Fig. 3). It is recalled that the velocity $v(x)$ is supposed to be periodic in x. The analysis is restricted furthermore to cases where minima and maxima are unique. The O points correspond to $w(x, k_x) = -v_+$, while the separatrix is defined by $w(x, k_x) = -v_-$. Hence the trapped wave domain is determined by the condition $-v_+ \leq w \leq -v_-$. In absence of dissipation $\mathcal{D}[N] = 0$, the action density is a function of w and σ only, where σ is the sign of k_x. For small and finite dissipation, it makes sense to solve the wave kinetic equation Eq.(6) by searching functions of (w, x, σ), instead of (x, k_x), i.e.

$$-C_k k_y k_x \frac{\partial N}{\partial x} = \mathcal{D}\left[N\right] \tag{13}$$

where $k_x(x, w, \sigma) = \sigma\sqrt{2\left(w + v(x)\right)}$. For a small enough dissipation rate, Eq.(13) can be solved perturbatively

$$N(w, x, \sigma) = N_0(w, \sigma) + \epsilon_D N_1(w, x, \sigma) + ... \tag{14}$$

where ϵ_D is an expansion parameter that depends on the details of the operator $\mathcal{D}\left[N\right]$. For the specific case of a diffusion operator, the expansion parameter is

$$\epsilon_D = \frac{D_k}{C_k k_y (v_+ - v_-)^{3/2}}$$

where D_k is the diffusion coefficient in k_x. The first order yields

$$-C_k k_y k_x \frac{\partial N_1}{\partial x} = \mathcal{D}\left[N_0\right]$$

After a division by k_x, and integration in x over a staircase period L, a solvability constraint is derived that determines N_0

$$\oint \frac{dx}{L} \frac{1}{k_x} \mathcal{D}\left[N_0\right] = 0 \tag{15}$$

where the integral is performed over a whole period of the wave position motion. The solvability constraint Eq.(15) bears an attractive form when the wave-wave interaction operator is written as the derivative of a flux Γ

$$\mathcal{D}[N] = \frac{\partial \Gamma}{\partial k_x} = k_x \frac{\partial \Gamma(x,w,\sigma)}{\partial w} \tag{16}$$

Eq.(15) becomes a condition of constant average flux $\langle \Gamma \rangle = \Gamma_0$, where the average flux is defined as

$$\langle \Gamma(x,w,\sigma) \rangle = \oint \frac{dx}{L} \Gamma(x,w,\sigma) \tag{17}$$

For passing waves $-v_- < w < +\infty$, the average flux reads

$$\langle \Gamma \rangle = \int_{-L/2}^{L/2} \frac{dx}{L} \Gamma(x,w,\sigma)$$

It depends on the Hamiltonian w and the sign σ of k_x. The constant Γ_0 is therefore different in the 2 passing domains $\sigma = \pm 1$. For trapped waves $-v_+ < w < -v_-$, the two branches $\sigma = \pm 1$ are connected, so that the average flux becomes

$$\langle \Gamma \rangle = \int_{-x_0(w)}^{x_0(w)} \frac{dx}{L} \left[\Gamma(x,w,-1) - \Gamma(x,w,+1) \right]$$

and depends on w only. Obviously $\langle \Gamma \rangle$ vanishes for a flux even in σ, $\langle \Gamma_{even} \rangle = 0$. The value of Γ_0 is different in the the 2 passing domains $w > -v_-$, $\sigma = \pm 1$ and the trapped domain $-v_- < w < -v_+$.

The gradient of N_0 has to match its unperturbed value $\partial_{k_x} N_{eq}|_{\mathbf{k}=\bar{\mathbf{k}}}$ far away from the island. This condition is hardened by requesting that the profile of N_0 itself joins smoothly its unperturbed value at infinity. In most cases, the value of the wave action density at the resonant surface $\bar{\mathbf{k}}$ can be removed from N_0 since it does not contribute to a Poisson bracket, nor to the wave-wave interaction operator when it is diffusive. The density N can then be shifted, and replaced by $N - N_{eq}\left(\bar{\mathbf{k}}\right)$. With these conventions, N_0 is typically an odd function of k_x in the passing domain $w > -v_-$, and an even function of k_x in the trapped domain (see Fig.4).

4 Radial structure of zonal flows

4.1 Calculation of the zonal force

The solution of Eq.(13) is used to compute the force Eq.(5). In [44], the shape of N_0 was chosen on the basis of general considerations and constraints. However this

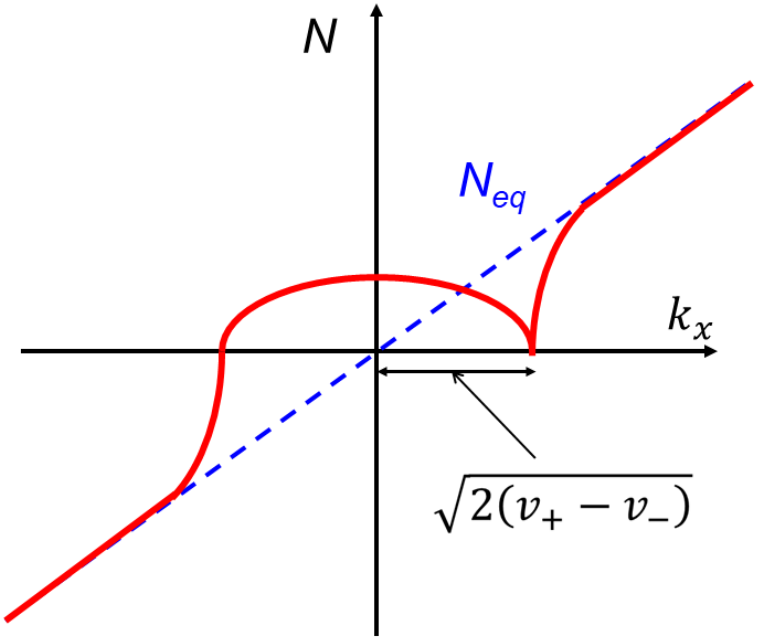

Figure 4: Schematic wave action profile near an island.

shape is determined by wave-wave non-linear interaction. In fact, the wave kinetic equation can be used to express the force vs the wave-wave interaction operator $\mathcal{D}[N]$ (still in the limit $k_x \ll k_y$)

$$\mathcal{F}(x) = -\int_{-\infty}^{+\infty} \frac{dk_y}{2\pi} \int_{-\infty}^{+\infty} \frac{dk_x}{2\pi} \mathcal{D}[N_0] \tag{18}$$

Since N_0 is known as a function of (w, σ), a change of variable from k_x to (w, σ) seems a natural course of action. The first step consists in reducing the integration in Eq.(18) over positive values k_x. This is readily done by decomposing the operator $\mathcal{D}[N_0]$ in odd and even components in k_x noted $\mathcal{D}_{odd}[N_0]$ and $\mathcal{D}_{even}[N_0]$ - obviously only the even part contributes. A change of variable $k_x \to w$ can then be done for $\sigma = +1$. The lower bound $k_x = 0$ corresponds to $w = -v$ at fixed x, while the separatrix is set by the condition $w = -v_-$ (see Fig.5). The zonal force then becomes

$$\mathcal{F}(x) = \int_{-\infty}^{+\infty} \frac{dk_y}{4\pi^2} I_k(x) \tag{19}$$

where I_k is an "intensity" equals to

$$I_k(v) = -2\int_{-v}^{+\infty} \frac{dw}{\sqrt{2\,(w+v)}} \mathcal{D}_{even}\left[N_0\right] \tag{20}$$

and $\mathcal{D}_{even}\left[N_0\right]$ is calculated on the $\sigma = +1$ branch (positive k_x). The function N_0 depends on the energy w only. Moreover it is anticipated that the operator $\mathcal{D}_{even}$ involves only explicit dependences on k_x - this is the case for all the model operators that are considered here. It then appears that the dependence on x of $\mathcal{D}_{even}\left[N_0\right]$ comes from the zonal velocity $v(x)$ [52]. In other words, $\mathcal{D}_{even}\left[N_0\right]$ is a function of (w, v, σ). The intensity thus depends on x via its dependence on v. The shape of $N_0(w)$ is expected to change rapidly near the separatrix $w = -v_-$, so that $\mathcal{D}\left[N_0\right]$ should be some localised function of argument $w + v_-$, up to some slow dependence on the flow minimum v_-. The intensity Eq.(20) can then be reformulated as a function $I_k\left(v_-, v - v_-\right)$. Finally, the intensity I_k is the sum of trapped and passing contributions $I_{k,t}$ and $I_{k,p}$, which are calculated by splitting the integration domain of Eq.(20) in two intervals $[-v, -v_-]$ and $[-v_-, +\infty]$ (see Fig.5).

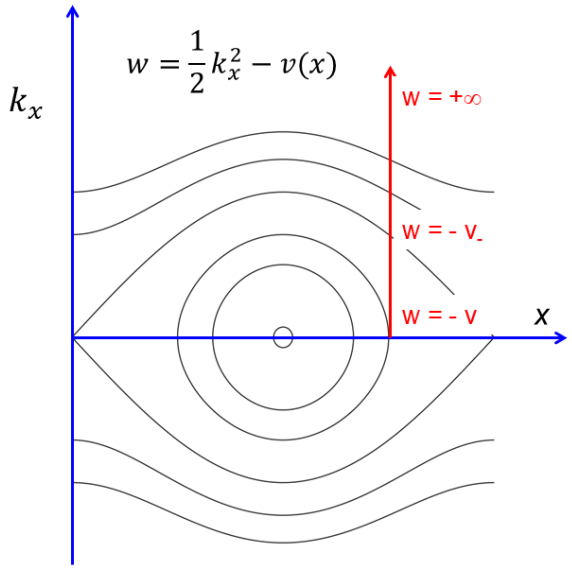

Figure 5: Change of variables $k_x \to w$ at fixed x.

4.2 Solution of the force balance equation

A close inspection of the force Eq.(19) indicates that it depends on x via a dependence on the velocity $V - V_-$ that can be singular (in the sense of an infinite derivative at $V = V_-$), parametrised by V_- (it is reminded that $v = V/C_k$, and $C_k > 0$). Hence the steady form of the force balance equation Eq.(4) reads

$$\mu \frac{d^2V}{dx^2} - \nu V + \mathcal{F}\left(V_-, V - V_-\right) = 0 \tag{21}$$

Introducing a shifted velocity $U = V - V_-$ and a normalised radial coordinate $\rho = \sqrt{\frac{2}{\mu}}x$, a first integral appears to be

$$\left(\frac{dU}{d\rho}\right)^2 + \Psi\left(V_-, U\right) = 0 \tag{22}$$

where

$$\Psi(V_-, U) = -\frac{\nu}{2}U^2 - \nu V_- U + \int_0^U dU'\, \mathcal{F}\left(V_-, U'\right) \tag{23}$$

is a "zonal potential". The constant of integration is fixed by the condition $\partial_\rho U = 0$ at $V = V_-$ (i.e. $U = 0$) since V_- is a minimum of the velocity $V(x)$. Eq.(22) is readily integrated to provide a formal solution

$$\rho = \pm \int_0^U \frac{dU'}{\sqrt{-\Psi\left(V_-, U'\right)}} \tag{24}$$

4.3 Existence and typology of solutions

Some general results can be obtained depending on the zonal force dependence on flow velocity.

Existence of periodic solutions. From Eq.24, it appears that solutions exist if $\Psi\left(V_-, U\right) < 0$ in some range of U values. When combined with Eq.(23), this constraint tells us that the force $\mathcal{F}(U)$ should be positive in some domain in U for a zonal flow to develop. It is thus instructive to study the potential Ψ near $U = 0$ (i.e. near the separatrix).

- A first possibility, called "type I force", is that $\mathcal{F}(U)$ is *positive* near $U = 0$ (an example is shown on Fig.6, left panel). For a well behaved force $\mathcal{F} \sim U^\alpha$ with $\alpha > 0$, the zonal contribution to the potential Ψ behaves as $\int_0^U dU'\, \mathcal{F}\left(V_-, U'\right) \sim U^{\alpha+1}$. It is sub-dominant compared with the viscous

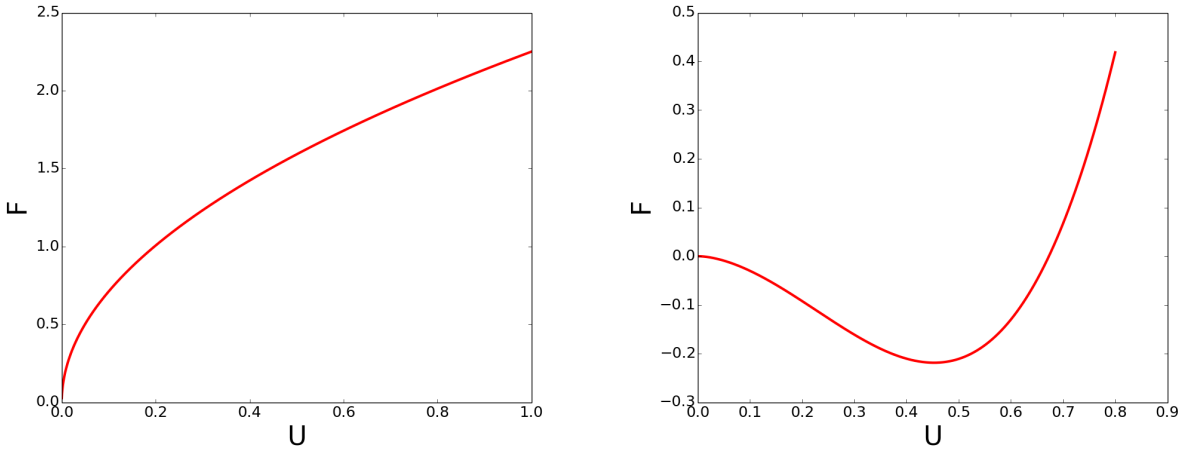

Figure 6: Left panel: example of type I zonal force $\mathcal{F}(U) = \frac{3}{2}\kappa U^{1/2}$ with $\kappa = 3/2$. Right panel: example of type II zonal force $\mathcal{F}(U) = -\alpha U^{\alpha} + 2\alpha U^{2\alpha}$ with $\alpha = 7/4$.

contribution $-\nu V_- U$, which thus prevails. The condition $\Psi < 0$ for the existence of a solution therefore requires that $V_- > 0$. When U increases, the potential reaches a minimum, then increases until it gets positive beyond some value $U = U_m$ (Fig. 7).

- A second possibility, called "type II force", is that $\mathcal{F}(U)$ is *negative* near $U = 0$, and becomes positive for larger values of U (see example on Fig.6, right panel), so that $\Psi(U)$ is again negative in a range $[0\,,\,U_m]$ (Fig. 8). In that case, solutions exist even with a null collisional friction coefficient $\nu = 0$.

In all cases the range of integration in Eq.(24) must be restricted to the interval $[0\,,\,U_m]$. Hence the second zero U_m of the zonal potential Ψ determines the range of zonal flow velocities

$$V_+ - V_- = U_m \tag{25}$$

Period and saturation level. The half-period in x is given by the condition

$$\sqrt{\frac{2}{\mu}}\frac{L}{2} = \int_0^{U_m} \frac{dU}{\sqrt{-\Psi\left(V_-, U\right)}} \tag{26}$$

Since the box size a should be a multiple n of L, this gives a relationship between $n = a/L$ and the saturation level V_-. The velocity range $U_m = V_+ - V_-$ then yields the zonal flow maximum V_+. Note that V_- is still unknown at this point. An additional condition is needed. One possible request is $V_- > 0$, a necessary

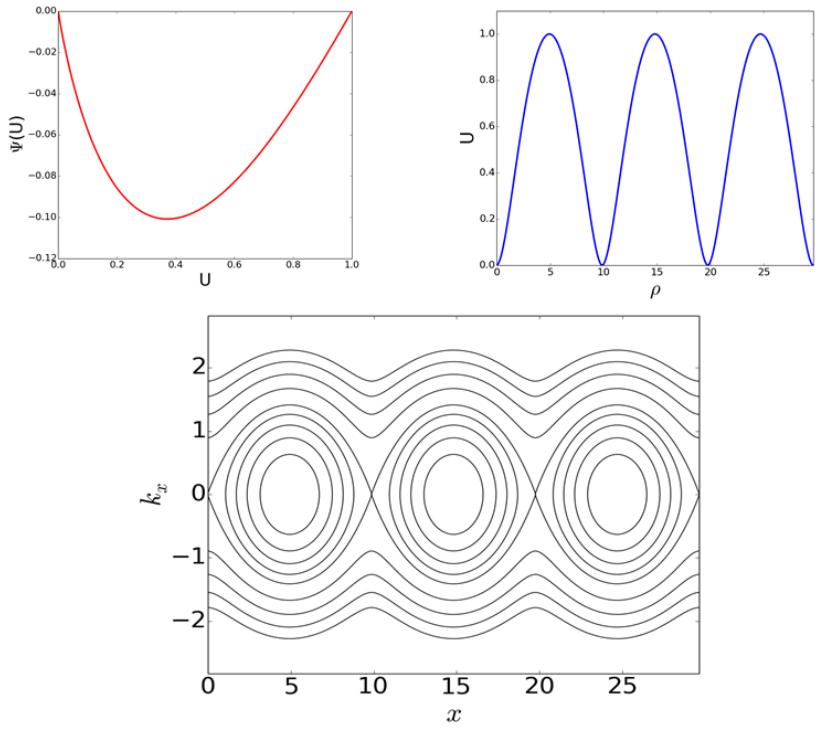

Figure 7: Contour lines of the reduced Hamiltonian w in the wave phase space (x, k_x), for a type I zonal force given by a Krook operator. The zonal force is $\mathcal{F}(U) = \frac{3}{2}\kappa U^{1/2}$ with $\kappa = 3/2$. The collisional friction coefficient is $\nu = 1$. The upper left small panel shows the zonal potential $\Psi(U)$. The radial profile over one period of the zonal velocity $U = V - V_-$ is shown in the upper right panel.

condition for finding viable solutions for type I zonal forces. It may rather be a poloidal momentum conservation constraint

$$\int_{-L/2}^{L/2} d\rho V(\rho) = 0 \tag{27}$$

This condition makes more sense from the physical point of view (global momentum conservation), and was in fact used in [43] to find radially periodic zonal flows. Momentum conservation imposes that $V_- < 0$, and thus allows type II forces only. The 3 conditions Eqs.(25,26,27) fully determine a "staircase" zonal flow solution.

Behaviour near X points. It is instructive to analyse the shape of the separatrix $W = -V_-$ near the X point, i.e. the curve $1/2C_k k_x^2 = U$ near $U = V - V_- = 0$. If the potential Ψ behaves as U^β, then $U \sim x^{\frac{2}{2-\beta}}$ and $k_x \sim x^{\frac{1}{2-\beta}}$ near an X point.

For type I forces, the friction term $-\nu V_- U$ controls the shape of Ψ and therefore $\beta = 1$. In that case, $k_x \sim x$ at the X point, so that the separatrix lines cross each other with a finite angle. On the other hand, for type II forces and $\nu = 0$, the parameter β is fully determined by the shape of the zonal force $\mathcal{F} \sim U^\alpha$, which implies $\beta = \alpha + 1$. If β approaches 2, i.e $\alpha \to 1$, the separatrix gets flat near the X point.

Behaviour near O points. The O point is analysed by considering values of W near $-V_+$, i.e. $W = -V_+ + \epsilon^2$, with $\epsilon \ll 1$. A Taylor development of Ψ near $U = U_m$ gives $\Psi = \Psi'_+ (U - U_m)$, with $\Psi'_+ = \frac{d\Psi}{dU}\big|_{U=U_m} > 0$. A solution of Eq.(24) yields

$$V = V_+ - 4\Psi'_+ \left(\rho - \frac{L}{2}\right)^2$$

and

$$\frac{1}{2} C_k k_x^2 + 4\Psi'_+ \left(\rho - \frac{L}{2}\right)^2 = \epsilon^2$$

Hence trajectories remain elliptic near the O point unless the zonal potential derivative vanishes $\Psi'_+ = 0$, which is unlikely. The O point is therefore "robust", unlike the X point, where the separatrix lines may flatten. A velocity profile that is flat near its minima (X points), and remains parabolic near its maxima (O point) is reminiscent of the staircase velocity bumps sometimes seen in simulations. Examples of type I and II zonal forces are shown on Figs. 7 and 8 (right panels).

5 Wave-wave diffusion operator with drive

5.1 Solution of the wave kinetic equation

As mentioned before, there is some arbitrariness in the choice of the wave-wave interaction operator $\mathcal{D}[N]$. In [52], 3 types of operators have been investigated: Krook operator, diffusive operator with or without a drive term. It appears that the Krook and diffusive operators share several common features: the action density $N_0(w, \sigma)$ is flat within the island (the trapped domain), while its gradient is singular near the separatrix. Moreover $N_0(w, \sigma)$ is an odd function of σ, hence of k_x. Since these operators conserve parity, they are also odd functions of σ and thus do not contribute to the zonal force. Hence a new ingredient is needed. It is provided by the growth rate of drift waves which add a source term to the r.h.s. of the wave kinetic equation. Indeed the resulting wave action density $N_0(w)$ is even in k_x within the island since both branches $\sigma = \pm 1$ are connected on a curve $w = cte$. It thus produces a non zero contribution to the zonal force in the trapped

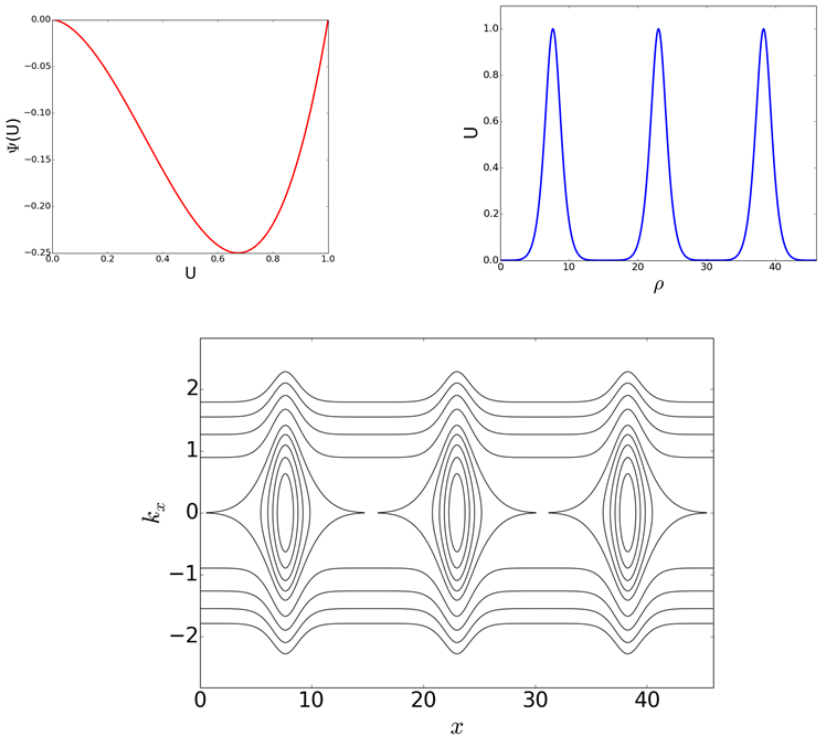

Figure 8: Contour lines of the reduced Hamiltonian w in the wave phase space (x, k_x), for a type II zonal force. The zonal force is $\mathcal{F}(U) = -\alpha U^{\alpha} + 2\alpha U^{2\alpha}$ with $\alpha = 7/4$. The collisional friction coefficient is $\nu = 0$. The upper left small panel shows the zonal potential $\Psi(U)$. The radial profile over one period of the zonal velocity $U = V - V_{-}$ is shown in the upper right panel.

domain. In this regard it is useful to reformulate the zonal force in a more tractable form. Following Eq.(16), the operator $\mathcal{D}[N]$ is written as a derivative of a flux Γ. The latter can be split in odd and even parts in k_x - only the odd part contributes. Also Γ can be chosen null at $k_x = 0$ since a constant can always be removed safely. The intensity I_k Eq.(20) can then be reformulated as

$$I_{k,t}(v) = -2\Gamma_{odd}\left(v, \sqrt{2\left(v - v_{-}\right)}\right) \tag{28}$$

The wave-wave interaction operator is now chosen of the form

$$\mathcal{D}[N] = \frac{\partial}{\partial k_x}\left(D_k \frac{\partial N}{\partial k_x}\right) + 2\gamma(\mathbf{k})N(x, \mathbf{k})$$

where $\gamma(\mathbf{k})$ is the drift wave growth rate. The wave action N can be replaced by is unperturbed value $N_{eq}(k_x, k_y)$, assuming that $\left(v_{+} - v_{-}\right)\gamma\left(\bar{\mathbf{k}}\right)/D_k \sim \epsilon_D$, where ϵ_D

is the expansion small parameter used in Eq.(14). The drive $2\gamma(\mathbf{k})N_{eq}(\mathbf{k})$, which acts as a source, is written as the derivative in k_x of a "flux" Φ_k such that

$$\Phi_k\left(k_x\right) = 2\int_0^{k_x} dq_x \gamma\left(q_x, k_y\right) N_{eq}\left(q_x, k_y\right)$$

The dependence on k_y is contained in the subscript k. The flux Φ_k can be written as a function (w, v, σ) by using the relation $k_x = \sigma\sqrt{2(w+v)}$. The total flux then reads

$$\Gamma(w, v, \sigma) = D_k k_x(w, v, \sigma)\frac{dN_0}{dw} + \Phi_k(w, v, \sigma)$$

The solvability constraint imposes

$$\frac{dN_0}{dw} = -\frac{1}{D_k}\frac{\langle\Phi_k\rangle(w)}{Q(w)}$$

where

$$Q(w) = \langle k_x\rangle = \oint \frac{dx}{L}\sqrt{2\left(w+v\right)}$$

and $\langle\Phi_k\rangle$ is the average of Φ_k as defined in Eq.(17). Note that $\langle\Phi_k\rangle\left(-v_+\right) = 0$ since $k_x = 0$ at the O-point and $\Phi_k(0) = 0$. Note also that only the odd part of Φ_k contributes to its average $\langle\Phi_k\rangle$. Finally the flux reads

$$\Gamma(w, v, \sigma) = -\frac{\langle\Phi_{k,odd}\rangle(w)}{Q(w)}\sigma\sqrt{2\left(w+v\right)} + \Phi_k(w, v, \sigma)$$

5.2 Zonal force with wave trapping and drive

Using Eq.(28), the intensity $I_{k,t}$ inside the island reads

$$I_{k,t}(v) = 2\frac{\langle\Phi_{k,odd}\rangle\left(-v_-\right)}{Q(-v_-)}\sqrt{2\left(v-v_-\right)} - 2\Phi_{k,odd}(\sqrt{2\left(v-v_-\right)})$$

where $\Phi_{k,odd}$ is the odd part of Φ_k in k_x restricted to $k_x > 0$. Using Eq.(19), the zonal force reads

$$\mathcal{F}(x) = 2\int_{-\infty}^{+\infty}\frac{dk_y}{4\pi^2}\left[\frac{\langle\Phi_{k,odd}\rangle\left(-v_-\right)}{Q(-v_-)}\sqrt{2\left(v-v_-\right)} - \Phi_{k,odd}(\sqrt{2\left(v-v_-\right)})\right]$$

If $\Phi_{k,odd}$ is negative near $k_x = 0$, the zonal force $\mathcal{F}$ is of type II and a staircase solution becomes possible. This condition can be made more explicit by using a Taylor development of γN_{eq} near $k_x = 0$

$$\gamma(\mathbf{k})N_{eq}(\mathbf{k}) = N_k\gamma_k\left[1 + 2\beta_k k_x + 3\lambda_k k_x^2 + o\left(k_x^3\right)\right]$$

where N_k and γ_k are respectively the wave action density and the growth rate calculated at $k_x = 0$. The constant term does not contribute to the zonal force because the corresponding flux Φ_k is linear in k_x and vanishes since $\langle \Phi_k \rangle = Q = \langle k_x \rangle$. The second term is odd in k_x, and thus provides a contribution to Φ_k that is even, which does not contribute to the zonal force. Hence only the quadratic term (and higher even orders) participate in the zonal force. If this term is the only one kept, the function $\Phi_k(k_x)$ is equal to $N_k \gamma_k \lambda_k k_x^3$, so that the zonal force becomes

$$\mathcal{F} = 4\sqrt{2}\frac{R(-v_-)}{Q(-v_-)}\int_{-\infty}^{+\infty}\frac{dk_y}{4\pi^2}\frac{\lambda_k}{C_k^{1/2}}N_k\gamma_k\left(V-V_-\right)^{1/2} \tag{29}$$

$$- \quad 8\sqrt{2}\int_{-\infty}^{+\infty}\frac{dk_y}{4\pi^2}\frac{\lambda_k}{C_k^{3/2}}N_k\gamma_k\left(V-V_-\right)^{3/2} \tag{30}$$

where

$$R(w) = \oint \frac{dx}{L}k_x^3 = 2\int_{-x_0(w)}^{x_0(w)}\frac{dx}{L}\left[2\left(w+v\right)\right]^{3/2}$$

The corresponding action density gradient within the island is given by the relation

$$\frac{dN_0}{dw} = -2N_k\gamma_k\frac{\lambda_k}{D_k}\frac{R(w)}{Q(w)}$$

An example of solution is shown on Fig.9. It then appears immediately that a staircase solution emerges when $\lambda_k < 0$. In the case where the growth rate varies more rapidly in k_x than the wave action density, this corresponds to the case where the growth rate is maximum at $k_x = 0$, a reasonable condition. In the case $\lambda_k < 0$, the force is of the form

$$\mathcal{F} = -\frac{3}{2}\kappa(V_-)\left(V-V_-\right)^{1/2} + \frac{5}{2}\tau\left(V-V_-\right)^{3/2}$$

with $\kappa, \tau > 0$. The numerical factors $\frac{2}{3}$ and $\frac{2}{5}$ have been conveniently introduced to produce a compact expression of the potential

$$\Psi(V_-, V) = \int_{V_-}^{V} dV' \mathcal{F}(V') = -\kappa(V_-)\left(V-V_-\right)^{3/2} + \tau\left(V-V_-\right)^{5/2} \tag{31}$$

5.3 Numerical solution

The formal solution $\rho(V_-, U)$, as given by Eq.(24), can be computed numerically for a given zonal force $\mathcal{F}$ and corresponding potential Ψ, and inverted to yield the

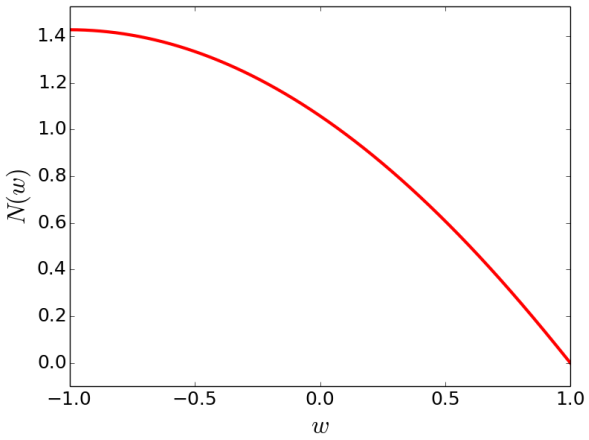

Figure 9: Wave action density for trapped waves versus reduced Hamiltonian for a wave-wave interaction operator that is diffusive plus drive. The zonal flow profile is $v(x) = cos(x)$, and $\lambda_k/D_k = 1.0$.

flow $V(\rho)$. The case of interest described in the previous section (diffusion and drive, plus wave trapping) gives a potential

$$\Psi(U) = -\kappa U^{3/2} + \tau U^{5/2}$$

The result is shown in Fig.10. The zonal potential $\Psi(U)$ is given by Eq.(31) with parameters $\kappa = 1, \tau = 1$. The friction parameter ν is set to 0. The force is of type II, and the zonal potential has an exponent $\beta = 1.5$. The island exhibits a separatrix that flattens (moderately) near the X point.

6 Discussion

6.1 Staircase solutions

Let us remind that we look for an idealised staircase solution consisting in a static quasi-periodic array of shear layers that bound areas where wave packets propagate radially. As mentioned before, Krook or diffusion operators do not provide acceptable solutions. It appears that a drive combined with diffusion does lead to a staircase-like solution, provided wave trapping is properly accounted for. This conclusion is also consistent with a poloidal momentum conservation constraint $\int d\rho V(\rho) = 0$. Indeed Krook and diffusion operators provide type I forces that do not allow negative values of velocity minima V_-. On the contrary the type II force found for a diffusion operator plus drive is consistent with negative values of V_-. Finally an analysis of the zonal flow velocity near the O and X points indicates

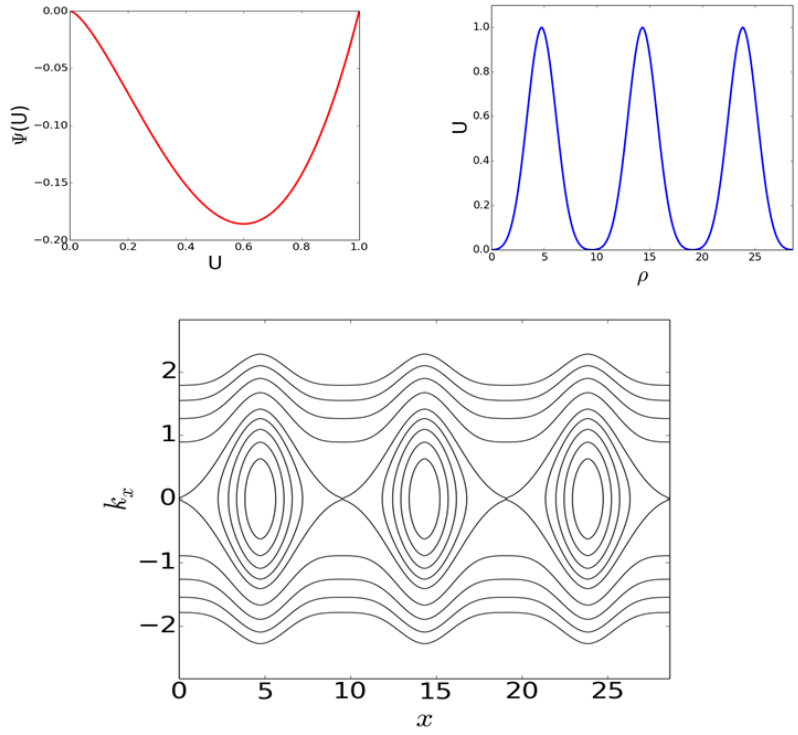

Figure 10: Contour lines of the reduced Hamiltonian w in the wave phase space (x, k_x) for the zonal potential computed with drive and a wave-wave interaction operator that is diffusive. The zonal force is $\mathcal{F}(U) = -\frac{3}{2}\kappa(V_-)\,(V-V_-)^{1/2} + \frac{5}{2}\tau\,(V-V_-)^{3/2}$ with $\kappa = 1$ and $\tau = 1$. The collisional friction coefficient is $\nu = 0$. The upper left small panel shows the zonal potential $\Psi(U)$. The radial profile over one period of the zonal velocity $U = V - V_-$ is shown in the upper right panel. The force is of type II and the separatrix flattens near the X point.

that non sinusoidal flows that are reminiscent of an idealised staircase, i.e. radial profiles of zonal flows that are peaked near their maximum and flat near their minimum, appear only in the case of diffusion plus drive. The flattest velocity profile near a velocity minimum is found for linear forces $\mathcal{F} \sim V - V_-$. This type of behaviour is hard to justify on the basis of the calculations above. More precisely it requires a diffusion coefficient D that goes like $|k_x|$, which seems unlikely. All these facts point towards a crucial role of finite growth rates and wave trapping. Incidentally the initial set of equations Eqs.(2,4,5) is identical to the one solved in [45], in the special limit where the GAM frequency vanishes and the wave-wave interaction operator reduces to a Krook operator plus drive. Though the case of a Krook operator plus drive is not investigated here, it appears that solutions of

this system exhibit common features with the present work, in particular a bump of the wave action density within the island in the case where the growth rate is maximum at $k_x = 0$ (see Fig.1, case $k_0 = 0$ in [45]).

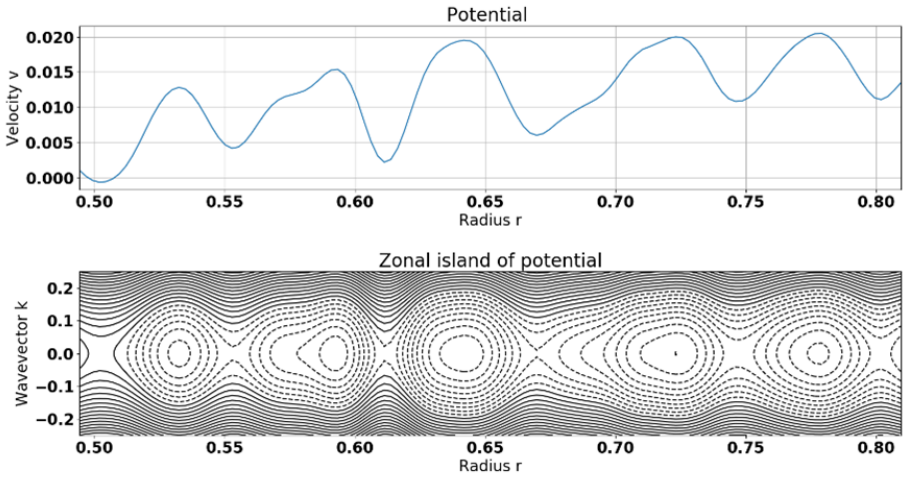

Figure 11: Top panel: radial profile of zonal flow velocity $V(x)$ from gyrokinetic simulations of ITG turbulence run with the GYSELA code. Lower panel: contour lines of the reduced Hamiltonian $w(x, k_x) = \frac{1}{2}k_x^2 - V(x)$. Parameters of the simulations are normalised ion gyroradius $\rho_* = 1/250$, collisionality $\nu_* = 0.14$, time average normalised gradient lengths $R_0/L_n = 1.62$ (variance 0.51) and $R_0/L_T = 5.66$ (variance 0.95) at mid-radius, safety factor $q(r) = 1.5 + 1.3\exp(2.5\log(r/a))$, aspect ratio $R_0/a = 3.2$ - details on conventions and normalisations can be found in [53].

6.2 Role of a mean shear flow

At this point, one conclusion is that staircase solutions are found in the case where the wave-wave interaction operator is diffusive, and the growth rate of drift waves is accounted for. A pending issue is the role of a mean flow, which appears in two places at least. One is the selection of a preferential direction in the propagation of avalanches, and the other is the condition for staircase formation. One difficulty though is to separate the mean flow from zonal flows, especially when all flows are nearly static, and without clear spatial scale separation. Let us note that in presence of gradients in a tokamak, the momentum equation Eq.(4) becomes

$$\frac{\partial V}{\partial t} = \mathcal{F} - \nu\,(V - V_{eq}) + \mu\frac{d^2V}{dx^2} \tag{32}$$

where V_{eq} is dictated by neoclassical physics. The total flow $V(x,t)$ can then be written as the sum of a "mean" flow $V_{eq}(x)$, in fact a large scale unperturbed flow,

and zonal flows. This definition is consistent with the procedure described in [20] where the mean flow is the flow before the emergence of a staircase. The mean flow $V_{eq}(x)$ then enters essentially the model via the unperturbed wave action density N_{eq} and Hamiltonian $H_{eq} = k_y V_{eq}(x,t)$.

6.2.1 Unperturbed wave action density

The complete calculation of the unperturbed wave action density in presence of a mean flow is beyond the scope of the present paper. One reason is that the notion of statistical equilibrium with shear flow and near marginality is tricky (see for instance the notions of "edge of chaos" for a model close to Hasewaga-Wakatani equations [54], or "transient growth" in a more elaborated model of turbulence in tokamaks [55]). A close topic is the calculation of the energy spectral density with shear flow. Examples of solutions can be found in [56, 57]. We illustrate here the main points with a simplified model where only the modification of the wave action density N_{eq} due to a mean flow is computed. The equation that rules the unperturbed wave action density N_{eq} is

$$-k_y \gamma_E \frac{\partial N_{eq}}{\partial k_x} = \mathcal{D}[N_{eq}, N_{eq}] + 2\gamma_{\mathbf{k}} N_{eq}$$

where $\gamma_E = \frac{\partial V_{eq}}{\partial x}$ is the shear flow rate, supposed constant, and $\mathcal{D}[N_{eq}, N_{eq}]$ is the full wave-wave interaction operator. In absence of drive and mean flow, the unperturbed wave action density is solution of the equation $\mathcal{D}[N_{eq}, N_{eq}] = 0$. As said, this is a difficult problem to solve. Models of non linear operator can be built, which predicts spectra in accordance with observations [56]. We look here for an approximate solution in the region $0 < k_x \ll k_y$, and we just look for the deformation of the wave action density, supposed of the form $N_{eq}(\mathbf{k}) = N_k \mathcal{N}(k_x)$. The wave kinetic equation is simplified as

$$-k_y \gamma_E \frac{\partial \mathcal{N}}{\partial k_x} = D_k \frac{\partial^2 \mathcal{N}}{\partial k_x^2} + 2\gamma_{\mathbf{k}} \mathcal{N}$$

where D_k is a diffusion coefficient that depends on some moment of the wave action density, say its value N_k at $k_x = 0$ for a given k_y. This is a rather crude model, in which D_k is merely a measure of the turbulence intensity N_k, while an additional local dependence on $\mathcal{N}$ would have been more realistic (but less tractable). The growth rate $\gamma_{\mathbf{k}}$ is expanded near $k_x = 0$

$$\gamma_{\mathbf{k}} = \gamma_k - \gamma_k'' k_x^2$$

The growth rate curvature γ_k'' is positive, in line with a growth rate maximum at $k_x = 0$. Solution is

$$N_{eq}(\mathbf{k}) = N_k \exp\left\{-\alpha_k \left(\frac{1}{2} k_x^2 - k_E k_x\right)\right\}$$

with the constraints

$$\alpha_k = \left(\frac{2\gamma_k''}{D_k}\right)^{1/2} \quad ; \quad k_E = -\frac{1}{2}\frac{k_y\gamma_E}{\left(2\gamma_k'' D_k\right)^{1/2}} \quad ; \quad D_k = \frac{2\gamma_k^2}{\gamma_k''}\left(1 - \frac{1}{8}\frac{k_y^2\gamma_E^2}{D_k\gamma_k}\right)^2 \tag{33}$$

The main effect of a mean flow shear is to shift the spectrum in k_x by a wave number k_E proportional to the shear rate, as expected [58, 59, 60, 61, 57]. As mentioned before, the diffusion coefficient D_k is some growing function of the turbulence intensity N_k. Hence the last bit of Eq.(33) can be seen as a saturation rule. For a small shear rate γ_E, an approximate expression is

$$D_k \simeq \frac{2\gamma_k^2}{\gamma_k''}\left(1 - \frac{1}{8}\frac{\gamma_k'' k_y^2\gamma_E^2}{\gamma_k^3}\right)$$

consistent with a decrease of the turbulent diffusion with shear rate [62, 63], and therefore a decrease of the turbulence spectral intensity N_k. Once a unperturbed solution has been found, consequences on avalanche propagation and staircase formation can be investigated.

6.2.2 Direction of avalanche propagation

Gyrokinetic simulations have shown in the past a preferential avalanche propagation correlated with the sign of the mean flow shear rate [64, 65, 20]. In the model proposed in [65], the avalanche propagation speed is given by the wave group velocity (in this case ITG modes in a tokamak plasma). The group velocity of drift waves is given by the relation

$$v_{g\mathbf{k}} = -\frac{k_x k_y}{\left(1 + k_x^2 + k_y^2\right)^2}$$

The shift k_E in Eqs.(33) can be seen as an average radial wave number k_x in the statistical sense. The corresponding mean group velocity is

$$v_{gk} \simeq \frac{1}{2}\frac{k_y^2}{\left(1 + k_y^2\right)^2}\frac{\gamma_E}{\left(2\gamma_k'' D_k\right)^{1/2}}$$

in the limit $k_y \gg k_x$. This estimate agrees well with numerical observations, i.e. an outward (inward) avalanche propagation speed for positive (negative) gradient of the radial electric field E_x (note that $V_{eq} = -E_x$ and thus $\gamma_E = -\frac{dE_x}{dx}$) [64, 65, 20]. This selective process, in which zonal and mean sheared flows add up or subtract to produce a preferential direction of avalanche propagation is similar to the one described in [20].

6.2.3 Impact on staircase formation

The role of a mean shear flow in view of the diffusion plus drive model is somewhat more intricate since it modifies the unperturbed wave action density $N_{eq}(\mathbf{k})$ that enters the Taylor development of $N_{\mathbf{k}}\gamma_{\mathbf{k}}$ Eq.(29). To avoid unnecessary complications, the calculation is limited to small values of k_E. An expansion yields the following expressions of the coefficients β_k, λ_k

$$\begin{aligned} \beta_k &= \frac{1}{2}\alpha_k k_E \\ \lambda_k &= -\frac{1}{3}\left[\frac{\gamma_k''}{\gamma_k} + \frac{1}{2}\alpha_k\left(1-\alpha_k k_E^2\right)\right] \end{aligned}$$

The shear rate of the mean flow has essentially an impact on the value of $\beta_k \sim k_y\gamma_E$. It was seen however that this parameter does not affect the zonal force Eq.(30) for parity reasons. Another effect of a mean shear flow is to make λ_k more positive. This shift does not favour the existence of staircase solution, keeping in mind the role of the sign of λ_k in Eq.(30). However this effect is small in the case where the growth rate curvature controls the value of λ_k. Hence the main effect of a mean shear flow appears to be a decrease of the turbulence intensity N_k. Looking at the structure of the zonal force Eq.(30), it is quite clear that its amplitude is inversely proportional to $N_k\gamma_k$. Decreasing the turbulence intensity N_k or the instability growth rate γ_k results in increasing the staircase period Eq.(26) as $(N_k\gamma_k)^{-1/2}$. A staircase cannot presumably survive if its spatial period is too small, as shear layers would likely interact and merge. A strong drive $N_k\gamma_k$ seems also inconsistent with a slowly evolving solution. This result, though somewhat stretched, is consistent with the common observation of staircases near instability threshold.

6.3 Link with gyrokinetic simulations

As a final word, let us stress that there is still a long way to an interpretation of gyrokinetic simulations of staircases in terms of wave trapping and flow erosion near X points.

The extension of this work to toroidal geometry, e.g. ITG modes in a tokamak, is beyond the scope of the present paper. However it is possible to give a hint of possible paths. A wave kinetic description in toroidal plasmas is allowed by the use of the ballooning representation framework [66, 67, 68, 69]. The radial wave number k_x then translates to the ballooning angle, and the coordinate x is the radial coordinate of the mode envelope, i.e. after an average over the fast radial variations near each resonant surface. A wave kinetic equation can be derived by using the variational technique described in [15]. An alternative path is to model

the evolution of a drift wave pump mode plus sidebands coupled to a zonal flow. This leads to a 4 wave model [6, 7], which can be reduced down to a 3 wave model for GAMs [8]. When applied to the Hasegawa-Mima equation, this approach leads to a system of 2 equations that rule a drift wave amplitude with a single wave number k_y to a zonal flow [70]. This system bears some similarities with the present model, though of course their meaning is different: in the approach [70] one mode only is looked after, whereas the wave kinetic approach describes a bath of modes. Interestingly soliton-like solutions are found, which can be loosely seen as counterparts to soliton/wave train solutions found with the wave kinetic equation when wave trapping is accounted for [44] - this methodology thus provides a description of avalanches coupled to zonal flows. The same procedure can be applied to the toroidal case based on the ballooning representation, with similar results, in particular envelope evolution equations of the non linear Schroedinger type. An overview can be found in [71]. However a proper application of this methodology to staircases remains to be demonstrated. In particular, one open question is whether solutions can be found in the spirit of the present work, i.e. an array of shear layers that surround regions of propagating solitons. A recent work suggests it is indeed the case [41].

Fig.11 comes from a simulation done with the GYSELA gyrokinetic code in a case where a staircase is present. It shows contour lines of the Hamiltonian $w(x, k_x)$ Eq.(7) with a zonal flow velocity $v(x)$ captured at a given time. All kinds of island shape are found in this snapshot, some with regular X points, others with flatter ones. In the spirit of the discussion above, this may be due to local differences in the growth rate vs the ballooning angle, though this remains speculative. One key question is whether the dynamics of ITG modes can be described by a wave kinetic equation, and more importantly whether wave trapping occurs. One noticeable fact is the observation of avalanches rebound on shear layers [34]. It has been found that wave trapping may explain the interplay between GAMs and turbulence background [45], and also the role of GAMs in avalanching [15]. Nevertheless a detailed analysis of the wave dynamics in actual 5D gyrokinetic simulations remains to be done.

Another feature of staircase patterns is the radial corrugation of the temperature [18], i.e. of the field that drives the underlying drift wave instabilities. In this regard, it is interesting to establish a connection with previous staircase models. It was found that feedback via density gradient plays a more important role than $E \times B$ shearing in models based on an Hasegawa-Wakatani model combined with a bistable mixing length [38, 39, 35]. Temperature relaxation plays also a central role in the model [20] since it is responsible for the onset of zonal flows, production of small scale eddies and subsequent avalanches via a transient realignment of the eddies. In the present model, density/temperature corrugations are not

computed. One may speculate though that density/temperature corrugations are merely a consequence of a local decrease of transport due to localised shear layers, some sort of micro-transport barriers. Temperature corrugations associated with staircase shear layers are documented in [34]. If so, an additional feedback loop may take place via the growth rate, which is presumably enhanced within the wave island. This may change in turn the properties of the zonal potential. It would however be premature to make a firm prediction without an accurate description of the modified growth rate.

Finally it seems that staircases are more easily observed close to marginality, more precisely close to the non linear turbulence threshold since ITG turbulence with adiabatic electrons response is characterised by a "Dimits" shift. To some extent, the present calculation is consistent with this property since a staircase solution requires both a positive growth rate and maximum negative curvature, suggesting a configuration with only a few unstable linear modes.

7 Conclusion

This work is an attempt to provide a description of a staircase pattern in gyrokinetic simulations. This description is based on a wave kinetic equation coupled to a zonal flow momentum equation. A staircase pattern is idealised as a periodic radial structure of zonal shear layers that bound regions of propagating wave packets, viewed as avalanches. Wave packets are trapped within shear layers due to refraction.

In the framework of wave kinetics, trapping is associated with the formation of an island in the wave phase space. For drift waves, a zonal flow maximum is generically associated with the island O point, while a flow minimum is an X point. Due to the wave-wave interaction operator, a singular layer appears near the island separatrix. This singular layer is the result of the boundary layer that inevitably appears to connect regions of propagating wave packets (avalanches) outside the island, and trapped waves within the island. A non linear solution of the wake kinetic equation can be constructed using a perturbative approach. This solution can then be injected in the momentum equation to compute the radial profile of zonal flows. This allows drawing general results on the existence and properties of solutions. Two types of zonal forces have been identified. The first one requires the presence of a collisional friction to provide an acceptable solution. The corresponding island exhibits a standard cat eye shape, i.e. finite angle X lines. The second type of solutions does not require any collisional friction. The island separatrix then exhibits a flattened X point, consistent with eroded flow minima. The detailed shape of the zonal potential depends sensitively on the boundary layer near the separatrix, hence on the choice of wave-wave interaction

operator. Since the theoretical (Boltzmann-like) wave-wave interaction operator is hardly tractable, model operators must be used to make progress. It appears that solutions with static periodic zonal flows are not found for simple Krook or diffusion operators. On the other hand, solutions do exist when a drive is added to the wave kinetic equation. This may reflect the fact that zonal flows cannot grow in the absence of unstable waves, in line with a predator-prey dynamics. Wave trapping plays an essential role in this case. These solutions exhibit eroded flows near their minima, in accordance with a feature sometimes observed in staircases. These eroded flows induce characteristic flat X points. Properties of the zonal force provide the difference between the flow maxima and minima, and the wave length versus the minimum zonal velocity. A third condition is needed to determine the latter. It appears that a condition of global momentum conservation eliminates zonal forces of the first type as contenders, hence reinforcing the conclusion that drive and wave trapping are necessary to find a staircase solution.

At this point, wave packets propagate in equal numbers in both radial directions. Asymmetry in propagation comes from a mean shear flow, which induces a finite radial wave number. "Mean" flow is to be understood here as radially coarse-grained, i.e. without the contribution from staircase shear layers. It also appears that a mean shear flow increases the spatial period of a staircase. Finally the entire study is handled for drift waves, whereas staircases were observed in gyrokinetic simulations of tokamak plasma turbulence. However most results may be extended to tokamak plasmas by mean of a ballooning representation, where the radial wave numbers are replaced by ballooning angles. This last point needs further verification and developments.

This model thus brings some elements of response to the list of questions raised in the introduction. A staircase pattern emerges from the interaction between propagating wave packets (avalanches) and waves that are trapped in zonal flow velocity wells. Amplitude, shape, and periodicity of the staircase pattern are determined by the background fluctuation spectra and growth rates. The zonal flow velocity radial profile is not sinusoidal, but tends to be localised near its radial maxima (O points). This is a consequence of the topological difference between O and X points. It appears that finite growth rates are essential for the build-up of this class of solutions. The optimum situation is a growth rate that is maximum at vanishing radial wave number. Finally a mean shear flow is needed to explain the preferential propagation speed of avalanches. It is not mandatory for the onset of a staircase, but it has an impact on its spatial period.

Acknowledgements
The authors acknowledge fruitful discussions with P. H. Diamond, Y. Kosuga and A. Ashourvan at the Festival of theory (Aix-en-Provence 2019 and 2021).

References

[1] Akira Hasegawa, Carol G. Maclennan, and Yuji Kodama. Nonlinear behavior and turbulence spectra of drift waves and rossby waves. *The Physics of Fluids*, 22(11):2122–2129, 1979.

[2] Akira Hasegawa and Masahiro Wakatani. Self-organization of electrostatic turbulence in a cylindrical plasma. *Phys. Rev. Lett.*, 59:1581–1584, Oct 1987.

[3] Z. Lin, T. S. Hahm, W. W. Lee, W. M. Tang, and R. B. White. Turbulent transport reduction by zonal flows: Massively parallel simulations. *Science*, 281(5384):1835–1837, 1998.

[4] P. H. Diamond, S-I. Itoh, K. Itoh, and T. S. Hahm. Zonal flows in plasma—a review. *Plasma Physics and Controlled Fusion*, 47(5):R35–R161, apr 2005.

[5] Diamond P. H., Rosenbluth M. N., Hinton F. L., Malkov M., Fleisher J., and Smolyakov A. Plasma physics and controlled nuclear fusion research. In IAEA-CN-69/TH3/1, editor, *17th IAEA Fusion Energy Conf.*, Vienna:IAEA, 1998.

[6] Liu Chen, Zhihong Lin, and Roscoe White. Excitation of zonal flow by drift waves in toroidal plasmas. *Physics of Plasmas*, 7(8):3129–3132, 2000.

[7] Liu Chen, Roscoe B. White, and F. Zonca. Zonal-flow dynamics and size scaling of anomalous transport. *Phys. Rev. Lett.*, 92:075004, Feb 2004.

[8] Z. Qiu, L. Chen, and F. Zonca. Excitation of kinetic geodesic acoustic modes by drift waves in nonuniform plasmas. *Physics of Plasmas*, 21(2):022304, 2014.

[9] Steven W. McDonald and Allan N. Kaufman. Weyl representation for electromagnetic waves: The wave kinetic equation. *Phys. Rev. A*, 32:1708–1713, Sep 1985.

[10] T.H. Stix. *Waves in Plasma*. New York: American Institute of Physics, 1992.

[11] P. H. Diamond, S-I. Itoh, and K. Itoh. *Modern Plasma Physics, vol. 1*. Cambridge University Press, 2010.

[12] D. E. Ruiz, J. B. Parker, E. L. Shi, and I. Y. Dodin. Zonal-flow dynamics from a phase-space perspective. *Physics of Plasmas*, 23(12):122304, 2016.

[13] Hongxuan Zhu, Yao Zhou, D. E. Ruiz, and I. Y. Dodin. Wave kinetics of drift-wave turbulence and zonal flows beyond the ray approximation. *Phys. Rev. E*, 97:053210, May 2018.

[14] Hongxuan Zhu, Yao Zhou, and I. Y. Dodin. Theory of the tertiary instability and the dimits shift from reduced drift-wave models. *Phys. Rev. Lett.*, 124:055002, Feb 2020.

[15] C. Gillot. *TBD*. Aix Marseille University, 2020.

[16] G. Dif-Pradalier, G. Hornung, Ph. Ghendrih, Y. Sarazin, F. Clairet, L. Vermare, P. H. Diamond, J. Abiteboul, T. Cartier-Michaud, C. Ehrlacher, D. Estève, X. Garbet, V. Grandgirard, Ö. D. Gürcan, P. Hennequin, Y. Kosuga, G. Latu, P. Maget, P. Morel, C. Norscini, R. Sabot, and A. Storelli. Finding the elusive $\mathbf{E} \times \mathbf{B}$ staircase in magnetized plasmas. *Phys. Rev. Lett.*, 114:085004, Feb 2015.

[17] F. Rath, A. G. Peeters, R. Buchholz, S. R. Grosshauser, P. Migliano, A. Weikl, and D. Strintzi. Comparison of gradient and flux driven gyro-kinetic turbulent transport. *Physics of Plasmas*, 23(5):052309, 2016.

[18] G. Dif-Pradalier, G. Hornung, X. Garbet, Ph. Ghendrih, V. Grandgirard, G. Latu, and Y. Sarazin. The exb staircase of magnetised plasmas. *Nuclear Fusion*, 57(6):066026, apr 2017.

[19] A. Weikl, A. G. Peeters, F. Rath, F. Seiferling, R. Buchholz, S. R. Grosshauser, and D. Strintzi. The occurrence of staircases in itg turbulence with kinetic electrons and the zonal flow drive through self-interaction. *Physics of Plasmas*, 25(7):072305, 2018.

[20] W. Wang, Y. Kishimoto, K. Imadera, J.Q. Li, and Z.X. Wang. A mechanism for the formation and sustainment of the self-organized global profile and exb staircase in tokamak plasmas. *Nuclear Fusion*, 58(5):056005, mar 2018.

[21] Lei Qi, Jae-Min Kwon, T.S. Hahm, Sumin Yi, and M.J. Choi. Characteristics of trapped electron transport, zonal flow staircase, turbulence fluctuation spectra in elongated tokamak plasmas. *Nuclear Fusion*, 59(2):026013, jan 2019.

[22] P. Ghendrih, Y. Asahi, E. Caschera, G. Dif-Pradalier, P. Donnel, X. Garbet, C. Gillot, V. Grandgirard, G. Latu, Y. Sarazin, S. Baschetti, H. Bufferand, T. Cartier-Michaud, G. Ciraolo, P. Tamain, R. Tatali, and E. Serre. Generation and dynamics of sol corrugated profiles. *Journal of Physics: Conference Series*, 1125(1):012011, 2018.

[23] P. G. Ivanov, A. A. Schekochihin, W. Dorland, A. R. Field, and F. I. Parra. Zonally dominated dynamics and dimits threshold in curvature-driven itg turbulence. *arXiv*, preprint 2004.04047, 2020.

[24] J. C. Hillesheim, E. Delabie, H. Meyer, C. F. Maggi, L. Meneses, E. Poli, and JET Contributors. Stationary zonal flows during the formation of the edge transport barrier in the jet tokamak. *Phys. Rev. Lett.*, 116:065002, Feb 2016.

[25] G. Hornung, G. Dif-Pradalier, F. Clairet, Y. Sarazin, R. Sabot, P. Hennequin, and G. Verdoolaege. $\mathbf{e}\times \mathbf{b}$ staircases and barrier permeability in magnetised plasmas. *Nuclear Fusion*, 57(1):014006, nov 2016.

[26] Minjun J. Choi, Hogun Jhang, Jae-Min Kwon, Jinil Chung, Minho Woo, Lei Qi, Sehoon Ko, Taik-Soo Hahm, Hyeon K. Park, Hyun-Seok Kim, Jisung Kang, Jaehyun Lee, Minwoo Kim, and Gunsu S. Yun and. Experimental observation of the non diffusive avalanche like electron heat transport events and their dynamical interaction with the shear flow structure. *Nuclear Fusion*, 59(8):086027, jun 2019.

[27] P. H. Diamond and T. S. Hahm. On the dynamics of turbulent transport near marginal stability. *Physics of Plasmas*, 2(10):3640–3649, 1995.

[28] B. A. Carreras, D. Newman, V. E. Lynch, and P. H. Diamond. A model realization of self organized criticality for plasma confinement. *Physics of Plasmas*, 3(8):2903–2911, 1996.

[29] X. Garbet and R. E. Waltz. Action at distance and bohm scaling of turbulence in tokamaks. *Physics of Plasmas*, 3(5):1898–1907, 1996.

[30] X Garbet, Y Sarazin, P Beyer, P Ghendrih, R.E Waltz, M Ottaviani, and S Benkadda. Flux driven turbulence in tokamaks. *Nuclear Fusion*, 39(11Y):2063–2068, nov 1999.

[31] Y. Sarazin and Ph. Ghendrih. Intermittent particle transport in two dimensional edge turbulence. *Physics of Plasmas*, 5(12):4214–4228, 1998.

[32] R Sanchez and D E Newman. Self-organized criticality and the dynamics of near-marginal turbulent transport in magnetically confined fusion plasmas. *Plasma Physics and Controlled Fusion*, 57(12):123002, nov 2015.

[33] T.S. Hahm and P.H. Diamond. Mesoscopic transport events and the breakdown of fick s law for turbulent fluxes. *Journal of the Korean Physical Society*, 73:747– 792, Sep 2018.

[34] Philippe Ghendrih, Claudia Norscini, Thomas Cartier-Michaud, Guilhem Dif-Pradalier, Jérémie Abiteboul, Yue Dong, Xavier Garbet, Ozgür Gürcan, Pascale Hennequin, Virginie Grandgirard, Guillaume Latu, Pierre Morel, Yanick Sarazin, Alexandre Storelli, and Laure Vermare. Phase space structures in gyrokinetic simulations of fusion plasma turbulence. *The European Physical Journal D*, 68(10):303, Oct 2014.

[35] Weixin Guo, Patrick H Diamond, David W Hughes, Lu Wang, and Arash Ashourvan. Scale selection and feedback loops for patterns in drift wave-zonal flow turbulence. *Plasma Physics and Controlled Fusion*, 61(10):105002, aug 2019.

[36] Y. Kosuga, P. H. Diamond, and Ö. D. Gürcan. How the propagation of heat-flux modulations triggers e x b flow pattern formation. *Phys. Rev. Lett.*, 110:105002, Mar 2013.

[37] Y. Kosuga, P. H. Diamond, G. Dif-Pradalier, and Ö. D. Gürcan. E x b shear pattern formation by radial propagation of heat flux waves. *Physics of Plasmas*, 21(5):055701, 2014.

[38] Arash Ashourvan and P. H. Diamond. How mesoscopic staircases condense to macroscopic barriers in confined plasma turbulence. *Phys. Rev. E*, 94:051202, Nov 2016.

[39] Arash Ashourvan and P. H. Diamond. On the emergence of macroscopic transport barriers from staircase structures. *Physics of Plasmas*, 24(1):012305, 2017.

[40] A. Hasegawa and M. Wakatani. Plasma edge turbulence. *Phys. Rev. Lett.*, 50:682–686, Feb 1983.

[41] A. Milovanov, J.J. Rasmussen, and Dif-Pradalier G. Avalanche transport from a nonlinear schroedinger model of the plasma staircases. *to be submitted*, 2020.

[42] A. I. Smolyakov, P. H. Diamond, and M. Malkov. Coherent structure phenomena in drift wave–zonal flow turbulence. *Phys. Rev. Lett.*, 84:491–494, Jan 2000.

[43] K. Itoh, K. Hallatschek, S.-I. Itoh, P. H. Diamond, and S. Toda. Coherent structure of zonal flow and onset of turbulent transport. *Physics of Plasmas*, 12(6):062303, 2005.

[44] P. Kaw, R. Singh, and P. H. Diamond. Coherent nonlinear structures of drift wave turbulence modulated by zonal flows. *Plasma Physics and Controlled Fusion*, 44(1):51–59, dec 2001.

[45] M. Sasaki, K. Itoh, T. Kobayashi, N. Kasuya, A. Fujisawa, and S.-I. Itoh. Propagation direction of geodesic acoustic modes driven by drift wave turbulence. *Nuclear Fusion*, 58(11):112005, oct 2018.

[46] A. Hasegawa and K. Mima. Stationary spectrum of strong turbulence in magnetized nonuniform plasma. *Phys. Rev. Lett.*, 39:205–208, Jul 1977.

[47] Jule G. Charney. Geostrophic Turbulence. *Journal of the Atmospheric Sciences*, 28(6):1087–1095, 09 1971.

[48] P. W. Terry and W. Horton. Drift wave turbulence in a low order k space. *The Physics of Fluids*, 26(1):106–112, 1983.

[49] R. E. Waltz. Numerical study of drift wave turbulence with simple models for wave wave nonlinear coupling. *The Physics of Fluids*, 26(1):169–179, 1983.

[50] Jeffrey B. Parker. Dynamics of zonal flows: failure of wave-kinetic theory, and new geometrical optics approximations. *Journal of Plasma Physics*, 82(6):595820602, 2016.

[51] Ira B. Bernstein, John M. Greene, and Martin D. Kruskal. Exact nonlinear plasma oscillations. *Phys. Rev.*, 108:546–550, Nov 1957.

[52] X. Garbet, O. Panico, R. Varennes, C. Gillot, G. Dif-Pradalier, Y. Sarazin, E. Bourne, V. Grandgirard, P. Ghendrih, D. Zarzoso, and L. Vermare. Proceedings of the international conference on the theory of fusion plasmas. *JPCS*, 2020.

[53] V. Grandgirard, J. Abiteboul, J. Bigot, T. Cartier-Michaud, N. Crouseilles, G. Dif-Pradalier, Ch. Ehrlacher, D. Esteve, X. Garbet, Ph. Ghendrih, G. Latu, M. Mehrenberger, C. Norscini, Ch. Passeron, F. Rozar, Y. Sarazin, E. SonnendrÃ¼cker, A. Strugarek, and D. Zarzoso. A 5d gyrokinetic full-f global semi-lagrangian code for flux-driven ion turbulence simulations. *Computer Physics Communications*, 207:35 – 68, 2016.

[54] Chris C. T. Pringle, Ben F. McMillan, and Bogdan Teaca. A nonlinear approach to transition in subcritical plasmas with sheared flow. *Physics of Plasmas*, 24(12):122307, 2017.

[55] M. Barnes, F. I. Parra, E. G. Highcock, A. A. Schekochihin, S. C. Cowley, and C. M. Roach. Turbulent transport in tokamak plasmas with rotational shear. *Phys. Rev. Lett.*, 106:175004, Apr 2011.

[56] Ö. D. Gürcan, X. Garbet, P. Hennequin, P. H. Diamond, A. Casati, and G. L. Falchetto. Wave number spectrum of drift-wave turbulence. *Phys. Rev. Lett.*, 102:255002, Jun 2009.

[57] G. M. Staebler, R. E. Waltz, J. Candy, and J. E. Kinsey. New paradigm for suppression of gyrokinetic turbulence by velocity shear. *Phys. Rev. Lett.*, 110:055003, Jan 2013.

[58] P. H. Diamond and Y.B. Kim. Theory of mean poloidal flow generation by turbulence. *Physics of Fluids B: Plasma Physics*, 3(7):1626–1633, 1991.

[59] R. E. Waltz, R. L. Dewar, and X. Garbet. Theory and simulation of rotational shear stabilization of turbulence. *Physics of Plasmas*, 5(5):1784–1792, 1998.

[60] P. W. Terry. Suppression of turbulence and transport by sheared flow. *Rev. Mod. Phys.*, 72:109–165, Jan 2000.

[61] X. Garbet, Y. Sarazin, P. Ghendrih, S. Benkadda, P. Beyer, C. Figarella, and I. Voitsekhovitch. Turbulence simulations of transport barriers with toroidal velocity. *Physics of Plasmas*, 9(9):3893–3905, 2002.

[62] C. F. Figarella, S. Benkadda, P. Beyer, X. Garbet, and I. Voitsekhovitch. Transport reduction by rotation shear in tokamak edge turbulence. *Phys. Rev. Lett.*, 90:015002, Jan 2003.

[63] F. L. Hinton and G. M. Staebler. Particle and energy confinement bifurcation in tokamaks. *Physics of Fluids B: Plasma Physics*, 5(4):1281–1288, 1993.

[64] Y. Idomura, H. Urano, N. Aiba, and S. Tokuda. Study of ion turbulent transport and profile formations using global gyrokinetic full-f vlasov simulation. *Nuclear Fusion*, 49(6):065029, may 2009.

[65] B. F. McMillan, S. Jolliet, T. M. Tran, L. Villard, A. Bottino, and P. Angelino. Avalanchelike bursts in global gyrokinetic simulations. *Physics of Plasmas*, 16(2):022310, 2009.

[66] John William Connor, R. J. Hastie, and John Bryan Taylor. High mode number stability of an axisymmetric toroidal plasma. *Proceedings of the Royal Society of London. A. Mathematical and Physical Sciences*, 365(1720):1–17, 1979.

[67] J. Y. Kim and M. Wakatani. Radial structure of high-mode-number toroidal modes in general equilibrium profiles. *Phys. Rev. Lett.*, 73:2200–2203, Oct 1994.

[68] F. Romanelli and F. Zonca. The radial structure of the ion temperature gradient driven mode. *Physics of Fluids B: Plasma Physics*, 5(11):4081–4089, 1993.

[69] Y Kishimoto, J-Y Kim, W Horton, T Tajima, M J LeBrun, and H Shirai. Toroidal mode structure in weak and reversed magnetic shear plasmas and its role in the internal transport barrier. *Plasma Physics and Controlled Fusion*, 41(3A):A663–A678, jan 1999.

[70] Zehua Guo, Liu Chen, and Fulvio Zonca. Radial spreading of drift wave zonal flow turbulence via soliton formation. *Phys. Rev. Lett.*, 103:055002, Jul 2009.

[71] Liu Chen and Fulvio Zonca. Physics of alfvén waves and energetic particles in burning plasmas. *Rev. Mod. Phys.*, 88:015008, Mar 2016.